

Thermodynamics of a quantum ring modified by Lorentz violation

A. A. Araújo Filho,^{1,*} H. Hassanabadi,^{2,†} J. A. A. S. Reis,^{3,4,‡} and L. Lisboa-Santos^{3,§}

¹*Departamento de Física Teórica and IFIC,*

*Centro Mixto Universidad de Valencia–CSIC. Universidad
de Valencia, Burjassot-46100, Valencia, Spain*

²*Physics Department, Shahrood University of Technology, Shahrood, Iran*

³*Programa de Pós-graduação em Física,*

*Universidade Federal do Maranhão (UFMA),
Campus Universitário do Bacanga, São Luís – MA, 65080-805, – Brazil*

⁴*Universidade Estadual do Sudoeste da Bahia (UESB),*

*Departamento de Ciências Exatas e Naturais,
Campus Juvino Oliveira, Itapetinga – BA, 45700-00, –Brazil*

(Dated: May 10, 2023)

Abstract

In this work, we investigate the consequences of Lorentz-violating terms in the thermodynamic properties of a 1-dimensional quantum ring. In particular, we use the ensemble theory to obtain our results of interest. The thermodynamic functions as well as the spin currents are calculated as a function of the temperature. We observe that parameter ξ , which triggers the Lorentz symmetry breaking, plays a major role in low temperature regime. Finally, depending on the configuration of the system, electrons can rotate in two different directions: clockwise and counterclockwise.

*Electronic address: dilto@fisica.ufc.br

†Electronic address: hha1349@gmail.com

‡Electronic address: jalfieres@gmail.com

§Electronic address: let.lisboa@hotmail.com

I. INTRODUCTION

The standard model extension (SME) [1–6] was created as an enlargement of the minimal standard model, possessing tensors which trigger the Lorentz symmetry breaking. Particularly, in its gauge sector, there exist much investigation in a variety of contexts [7–17], involving interactions of photon-fermion [18], nonminimal couplings [19], and operators of higher mass dimension [20]. Investigations focusing on the fermionic sector of the SME were correlated to the violation of CPT symmetry [21], which was a productive environment for the subsequent applications [12, 22–25].

Condensed matter systems represent a fruitful field for studying Lorentz symmetry breaking [26, 27], because there can exist privileged spacetime directions due to the tensor fields, leading a breakdown of rotation invariance. Two dimensional electronic systems form a remarkable environment worthy to be explored [28], where spin-orbit interaction has a relevant role, since there exists a correlation with the spintronics [29]. In this case, persistent currents and geometrical phases turn out to be observables.

A relevant feature when we deal with Lorentz violation, encoded by modified dispersion relations, is definitely its thermodynamic aspects. Studies concerning thermodynamic properties in Lorentz-violating scenarios could supply additional information about the primordial stages of the Universe [30]. The correlation between them was initially addressed in Ref. [31]. After that, many works have been proposed in the literature within different contexts, namely, Podolsky electrodynamics [32] and electrodynamics with an additive Myers–Pospelov term [33–35], graviton [36], CPT-even and CPT-odd violations [37–39], higher-dimensional operators [27], Einstein–eather theory [40], bouncing universe [41], and loop quantum gravity [42].

There are several works involving the study of quantum rings within different scenarios [43–49]. Additionally, a recent study appeared in the literature, focusing on the main classical aspects of 1-D quantum rings with Lorentz violation [50]. Nevertheless, up to now, there is a lack in the literature concerning an investigation of the thermodynamic properties of quantum rings in this latter context. Such examination is notable since it might possibly reveal different phenomena ascribed to a new physics, which might be detected in a future laboratory experiment. It is important to mention that, throughout of this manuscript, natural units have been used. This means, for instance, that the Boltzmann constant is set

to $k_B = 1$.

II. THERMODYNAMIC DESCRIPTION

Initially, we regard the general quadratic sector of a renormalizable CPT-violating Lagrangian, which describes a massive Dirac fermion

$$\mathcal{L} = \frac{i}{2} \bar{\psi} \Gamma^\nu \overleftrightarrow{\partial}_\nu \psi - \bar{\psi} M \psi, \quad (1)$$

with $\Gamma^\nu := \gamma^\nu + c^{\mu\nu} \gamma_\mu + d^{\mu\nu} \gamma_5 \gamma_\mu + e^\nu + i f^\nu \gamma_5 + g^{\mu\nu} \sigma_{\lambda\mu}/2$ and $M := m + a_\mu \gamma^\mu + b_\mu \gamma_5 \gamma^\mu + H^{\mu\nu} \sigma_{\mu\nu}/2$, where the gamma matrices have the conventional properties, i.e., $\mathbb{1}, \gamma_5, \gamma^\mu, \gamma_5 \gamma^\mu, \sigma^{\mu\nu}$. In addition, parameters $a_\mu, b_\mu, c_{\mu\nu}, H_{\mu\nu}$ are given by the vacuum expectation values of Lorentz tensors, which come from the spontaneous Lorentz-breaking of a more fundamental theory [51]. More so, the Hamiltonian from Eq. (1) can also be derived as

$$H = -A^\dagger \gamma^0 (i \Gamma^j \partial_j - M) A \quad (2)$$

where A is a non-singular matrix (not depending on the spacetime), which satisfy the condition below

$$A^\dagger \gamma^0 \Gamma^0 A = \mathbb{1}. \quad (3)$$

Now, let us consider the recent results in literature proposed by Ref. [50]. Mainly, there exists an effective nonrelativistic Hamiltonian

$$H = \frac{p^2}{2m} + d_{jk} p^j \sigma^k + d_{00} p^i \sigma^i, \quad (4)$$

which provides structures analogous to Rashba and Dresselhauss interactions. When the system is restricted to a 1-dimensional quantum ring, two main features give rise to: the appearance of geometrical phases and persistent spin currents effects. Fundamentally, they occur due to the operators d_{jk} and d_{00} . The respective energy eigenvalues are obtained as follows:

$$E_{n,s}^{d_{jk}} = \Omega \left\{ n - \frac{1}{2} \left[1 + (-1)^s \sqrt{1 + 4\xi^2} \right] \right\}^2, \quad (5)$$

$$E_{n,s}^{d_{00}} = \Omega \left\{ n + \frac{1}{2} \left[1 - (-1)^s \sqrt{1 + 4\xi_{00}^2} \right] \right\}^2, \quad (6)$$

where $n \in \mathbb{Z}$, $\Omega = 1/2mr_0^2$, $s = 1$ represents the energy for spin-down particles while $s = 2$ represents the energy for spin-up ones. The information about Lorentz violation relies on

the parameters $\xi = mr_0\sqrt{d_{12}^2 + d_{11}^2}$ and $\xi_{00} = mr_0d_{00}$, where m is the electron mass and r_0 is the radius of the quantum ring. It is important to mention that we have used $p_z = 0$, since electrons move on the plane. We have also set $d^{32} = d^{31} = d^{33} = 0$, so that d^{ij} becomes a 2×2 matrix. Choosing $d^{22} = -d^{11}$, tensor $d^{\mu\nu}$ becomes traceless, as required. Also, the components d^{0i} and d^{i0} are set to be zero because they do not fit with our purpose, the Rashba- and Dresselhauss-like interactions. From now on, we shall describe the properties of interest based on parameters ξ and ξ_{00} , instead of purely Lorentz-violating parameters themselves. We choose such a configuration due to the necessity of keeping both mass and radius fixed in order to vary the controlling coefficients only. It is worthy to be mentioned that the eigenstates were also calculated in Ref. [50]. Nevertheless, only with the spectral energy our main results of interest can be obtained. The spin current may be calculated for an arbitrary state as [50]

$$\mathcal{J}_\varphi^z = \frac{1}{4mr_0} (2n \cos \theta - 1), \quad (7)$$

where θ can assume the form of either $\theta = \arctan(2\xi)$ or $\theta = \arctan(2\xi_{00})$, i.e., if we consider d_{jk} or d_{00} respectively. In our work, we investigate the consequences of Lorentz-violating dispersion relations present in Eqs. (5) and (6) within the thermodynamic properties of a 1-dimensional quantum ring. To do so, we apply two different methods to study the thermal aspects of non-interacting electrons of our system.

The first method is based on the canonical ensemble formalism. On the other hand, the second one is founded on the grand canonical ensemble theory. These approaches allow us to study N electrons confined to a 1-dimensional quantum ring in contact with a thermal reservoir. Additionally, it is worth pointing out that using the first method, we are not able to take into account the Fermi-Dirac statistics since there does not exist the differentiation ascribed to the quantum number. Then, electrons are free to choose its accessible quantum states. However, for the second situation, we are able to take into account the Fermi-Dirac statistics.

In the canonical ensemble, it is well-known that the partition function is given by

$$\mathcal{Z} = \sum_{\{n_j\}} \exp(-\beta E_{\{n_j\}}), \quad (8)$$

where $\{n_j\}$ is related to all accessible quantum states. Since we are dealing with N non-

interacting particles, the partition function in Eq. (8) can be factorized [52, 53]

$$\mathcal{Z} = \mathcal{Z}_1^N = \left\{ \sum_{n=0}^{\infty} \sum_{s=1}^2 \exp(-\beta E_{n,s}) \right\}^N, \quad (9)$$

where we have defined the single partition function as

$$\mathcal{Z}_1 = \sum_{n=0}^{\infty} \sum_{s=1}^2 \exp(-\beta E_{n,s}). \quad (10)$$

In order to obtain an analytical expression for it, we use the *Euler–Maclaurin* formula [53–56]

$$\begin{aligned} \sum_{n=0}^{\infty} F(n) &= \int_0^{\infty} F(n) dn + \frac{1}{2}F(0) \\ &\quad - \frac{1}{2!}B_2F'(0) - \frac{1}{4!}B_4F'''(0) + \dots, \end{aligned} \quad (11)$$

where B_m are the Bernoulli numbers: $B_2 = 1/6$, $B_4 = -1/30$, \dots . Performing the calculations, we get

$$\begin{aligned} \mathcal{Z}_1^{d_{jk}} &= \sqrt{\frac{\pi}{\beta\Omega}} \left\{ 1 + \frac{1}{2} \sum_{s=1}^2 \text{Erf} \left[\sqrt{\frac{\beta\Omega}{4}} \Delta_s \right] \right\} + \\ &\quad \sum_{s=1}^2 \exp \left(-\frac{\beta\Omega}{4} \Delta_s^2 \right) \times \\ &\quad \times \left\{ \frac{1}{2} - \frac{\beta\Omega}{12} \left(1 + \frac{\beta\Omega}{10} \right) \Delta_s + \frac{\beta^3\Omega^3}{720} \Delta_s^3 + \dots \right\}, \end{aligned} \quad (12)$$

where we have defined

$$\Delta_s \equiv 1 + (-1)^s \sqrt{1 + 4\xi^2}, \quad (13)$$

$$\text{Erf}[z] = \frac{2}{\sqrt{\pi}} \int_0^z e^{-t^2} dt. \quad (14)$$

In particular, for the coefficient d_{00} , we find

$$\begin{aligned} \mathcal{Z}_1^{d_{00}} &= \frac{1}{2} \sqrt{\frac{\pi}{\beta\Omega}} \sum_{s=1}^2 \text{Erf} \left[\sqrt{\frac{\beta\Omega}{4}} \Psi_s \right] + \\ &\quad \sum_{s=1}^2 \exp \left(-\frac{\beta\Omega}{4} \Psi_s^2 \right) \times \\ &\quad \times \left\{ \frac{1}{2} + \frac{\beta\Omega}{12} \left(1 + \frac{\beta\Omega}{10} \right) \Psi_s - \frac{\beta^3\Omega^3}{720} \Psi_s^3 + \dots \right\}, \end{aligned} \quad (15)$$

where

$$\Psi_s \equiv 1 - (-1)^s \sqrt{1 + 4\xi_{00}^2}. \quad (16)$$

Here, we must take care about the convergence of the power series. In both Eq. (12) and (15), we can see the presence of an exponential in front of the power series. Such term is a function of temperature and, for the range that we choose to evaluate the thermodynamic functions, $0 < T < 1$ eV, it is possible to ensure the convergence of the partition functions and their respective thermodynamic quantities. Nevertheless, for a different range of temperatures, an additional study about the convergence must be carried out. It is important to mention that this examination lies beyond of the scope of this current work.

Moreover, the connection with the thermodynamics is given by the Helmholtz free energy

$$f = -\frac{1}{\beta} \lim_{N \rightarrow \infty} \frac{1}{N} \ln \mathcal{Z}, \quad (17)$$

where we write rather the Helmholtz free energy per particle. With this, we can derive the following thermodynamic state functions, i.e., entropy, heat capacity and mean energy respectively,

$$s = -\frac{\partial f}{\partial T}, \quad c = T \frac{\partial s}{\partial T}, \quad u = T^2 \frac{\partial}{\partial T} \ln \mathcal{Z}. \quad (18)$$

For the grand canonical ensemble, the grand partition function reads

$$\Xi = \sum_{N=0}^{\infty} \exp(\beta\mu N) \mathcal{Z}[N_{n,s}], \quad (19)$$

where $\mathcal{Z}[N_{n,s}]$ is the usual canonical partition function. Since we are dealing with fermions, the occupation number allowed for each quantum state is restricted to $N_{n,s} = \{0, 1\}$. So, for an arbitrary quantum state, the energy also depends of the occupation number as

$$E\{N_{n,s}\} = \sum_{\{n,s\}} N_{n,s} E_{n,s} \quad (20)$$

where we have

$$\sum_{\{n,s\}} N_{n,s} = N. \quad (21)$$

Therefore, the partition function becomes

$$\mathcal{Z}[N_n] = \sum_{\{N_{n,s}\}} \exp \left[-\beta \sum_{n=0}^{\infty} \sum_{s=1}^2 N_{n,s} E_{n,s} \right]. \quad (22)$$

The grand partition function assumes the form

$$\Xi = \sum_{N=0}^{\infty} \exp(\beta\mu N) \sum_{\{N_{n,s}\}} \exp \left[-\beta \sum_{n=0}^{\infty} \sum_{s=1}^2 N_{n,s} E_{n,s} \right], \quad (23)$$

which can be rewritten as

$$\Xi = \prod_n \prod_s \left\{ \sum_{N_{n,s}=0}^1 \exp[-\beta N_{n,s} (E_{n,s} - \mu)] \right\}. \quad (24)$$

Performing the sum over the two possible occupation numbers, we get

$$\Xi = \prod_n \prod_s \{1 + \exp[-\beta (E_{n,s} - \mu)]\}. \quad (25)$$

The connection with thermodynamics is made using the grand potential given by

$$\Phi = -\frac{1}{\beta} \ln \Xi. \quad (26)$$

Replacing Ξ , in above expression, we get

$$\Phi = -\frac{1}{\beta} \sum_{n=0}^{\infty} \sum_{s=1}^2 \ln \{1 + \exp[-\beta (E_{n,s} - \mu)]\}. \quad (27)$$

Despite we could apply the *Euler-Maclaurin* formula, the results are lengthy and not easy to comprehend their respective phenomenology. Therefore, for the sake of en-lighting our analysis, we provide numerical calculations. Also, we utilize the grand potential to calculate the thermodynamic quantities of interest: mean particle number, internal energy, entropy and heat capacity:

$$\mathcal{N} = -\frac{\partial \Phi}{\partial \mu}, \quad \mathcal{U} = -T^2 \frac{\partial}{\partial T} \left(\frac{\Phi}{T} \right), \quad S = -\frac{\partial \Phi}{\partial T}, \quad C = T \frac{\partial S}{\partial T}. \quad (28)$$

In order to calculate all thermodynamics quantities using both methods, we need to perform the sum present in Eqs. (10) and (27). Unfortunately, it is not possible to do so in a closed form to either cases. However, numerical analyses can be performed instead and we can acquire an idea of the behavior of all thermodynamic quantities, i.e., both in high and low temperature regimes. The next sections are devoted to study both configurations, namely d_{ij} and d_{00} , for a numerical viewpoint. For this propose, we use $r_0 = 50$ nm for the radius of the quantum ring [57, 58], $m = 0.511$ MeV for the electron mass and $\mu = 0.1$ eV for the chemical potential.

III. RESULTS FOR CANONICAL APPROACH

This section aims at presenting some numerical result concerning the canonical ensemble formalism. We intend to study the main thermodynamic functions, namely, the Helmholtz

free energy, internal energy, entropy and, finally, the heat capacity. In the following subsections, we present the results for two configurations, i.e., the d_{ij} and d_{00} . We finish this section showing how the z -component of the spin current behave for both configurations as a function of temperature.

A. Configuration d_{ij}

The plots displayed in Fig. 1 show the main thermodynamic quantities as a function of temperature. We are also free to choose values for the parameter ξ in order to comprehend how those quantities change. It is important to point out that we consider the low temperature regime the range $0 < T < 0.6$ eV and the high temperatures $T > 0.6$ eV.

Our investigation starts with the Helmholtz free energy shown in Fig. 1a. In this case, for temperatures relying on the range $0 < T < 0.6$ eV, we see that the free energy has its minimum when $\xi = 0$, and its maximum when $\xi = 0.9$. For $T > 0.6$ eV all curves tend to the same values. This feature is expected since, for high temperatures, Lorentz violating parameters turn out to be negligible. As the temperature increases, the Helmholtz free energy reaches negative values.

The internal energy is displayed in Fig. 1b. As before, for $\xi = 0.9$, we find the maximum value for the energy. For high temperatures, we obtain the plots in a such way that they converge to the same values. For low temperature regime, we see the most significant difference among the graphics. We observe that $\xi = 0.9$ give us the highest energy and, in the range $0 < \xi < 0.9$, the energy increases as the parameter ξ increases. It is interesting to notice that from $\xi > 1.0$ the internal energy decreases and the numerical analyses show us that it keeps decreasing as parameter ξ increases. The entropy showed in Fig. 1c has the same behavior, i.e., it has its maximum values bounded from $\xi = 0.9$, and for high temperature, Lorentz parameter plays no role.

We finish this subsection discussing the behavior of the heat capacity. As displayed in Fig. 1d, we observe that, for high temperatures, the parameter ξ plays no role in the value of the heat capacity since all plots converge to $\mathcal{C} = 0.5$. On the other hand, for low temperatures, we verify an interesting feature. For instance, for parameters $\xi = 0.6$ and $\xi = 0.9$, we have a local minimum at $T = 0.25$ eV. Moreover, for $\xi = 0$, we have a local maximum at $T = 0.4$ eV, and for $\xi = 0.3$, the local maximum behavior fades. For the ranges $0 < \xi < 0.9$

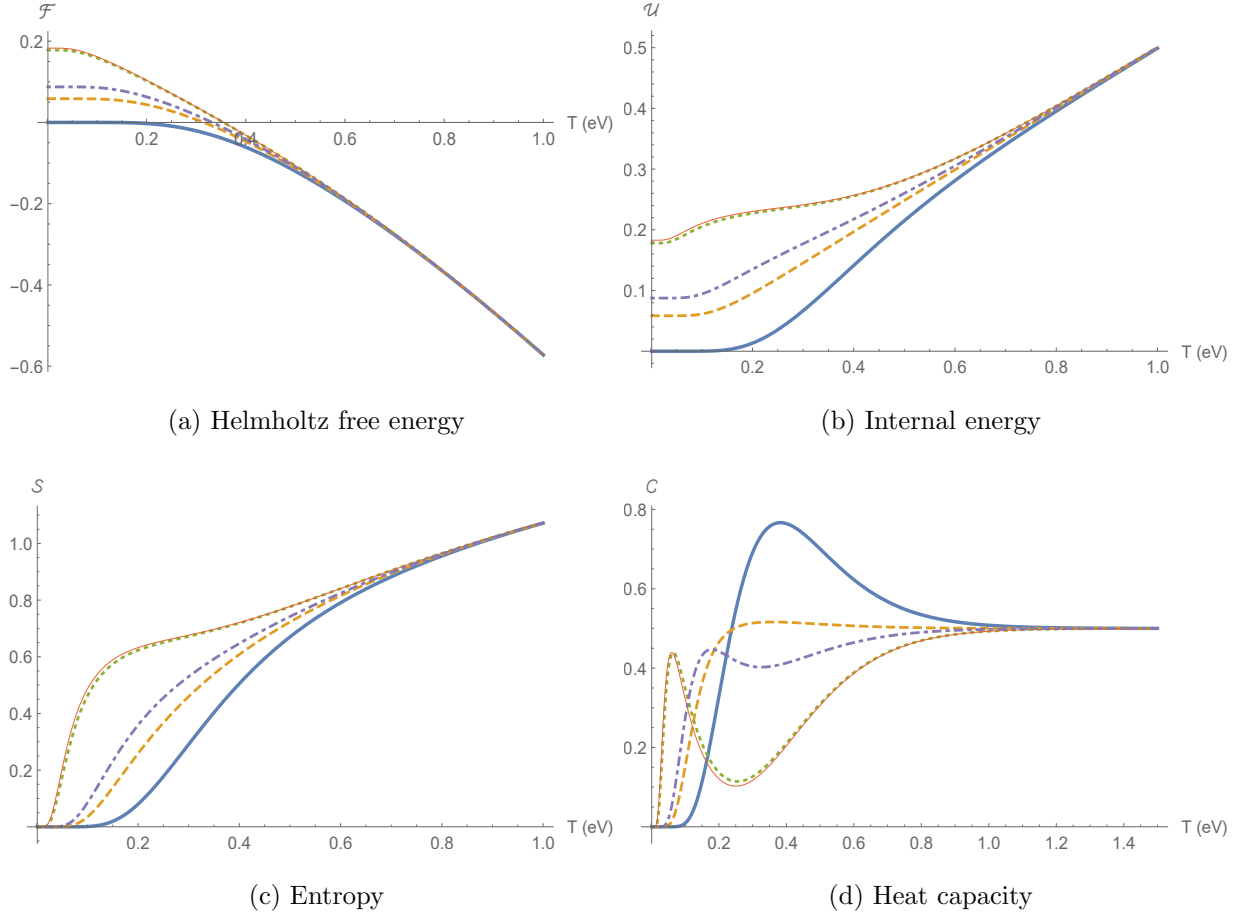


Figure 1: The main thermodynamic functions modified by the anisotropic parameter d_{ij} are displayed above. The plots can be distinguished by the following labels: (thick, blue, $\xi = 0.0$), (dashed, orange, $\xi = 0.3$), (dotted, green, $\xi = 0.6$), (thin, red, $\xi = 0.9$), (dotdashed, purple, $\xi = 1.2$). More so, the crossover to negative energies happens in larger temperatures for increasing $\xi \in [0, 0.9]$.

and $0.2 \text{ eV} < T < 0.4 \text{ eV}$, we observe a transitions between a local maximum to a local minimum. For $\xi > 0.9$, we see the formation of a new local maximum values in the range $0.15 \text{ eV} < T < 0.2 \text{ eV}$. For temperature below 0.15 eV , we see that both $\xi = 0.6$ and $\xi = 0.9$ have a local maximum at 0.05 eV , while for the other values of the parameter ξ , the heat capacity goes to zero.

B. Configuration d_{00}

In this subsection, we intend to study the modifications produced by the Lorentz violating parameter d_{00} . The plots displayed in Fig. 2 summarize the main thermodynamic quantities as a function of temperature. We also use the freedom of the parameter ξ_{00} in order to understand how the thermodynamic quantities change with both temperature and ξ_{00} .

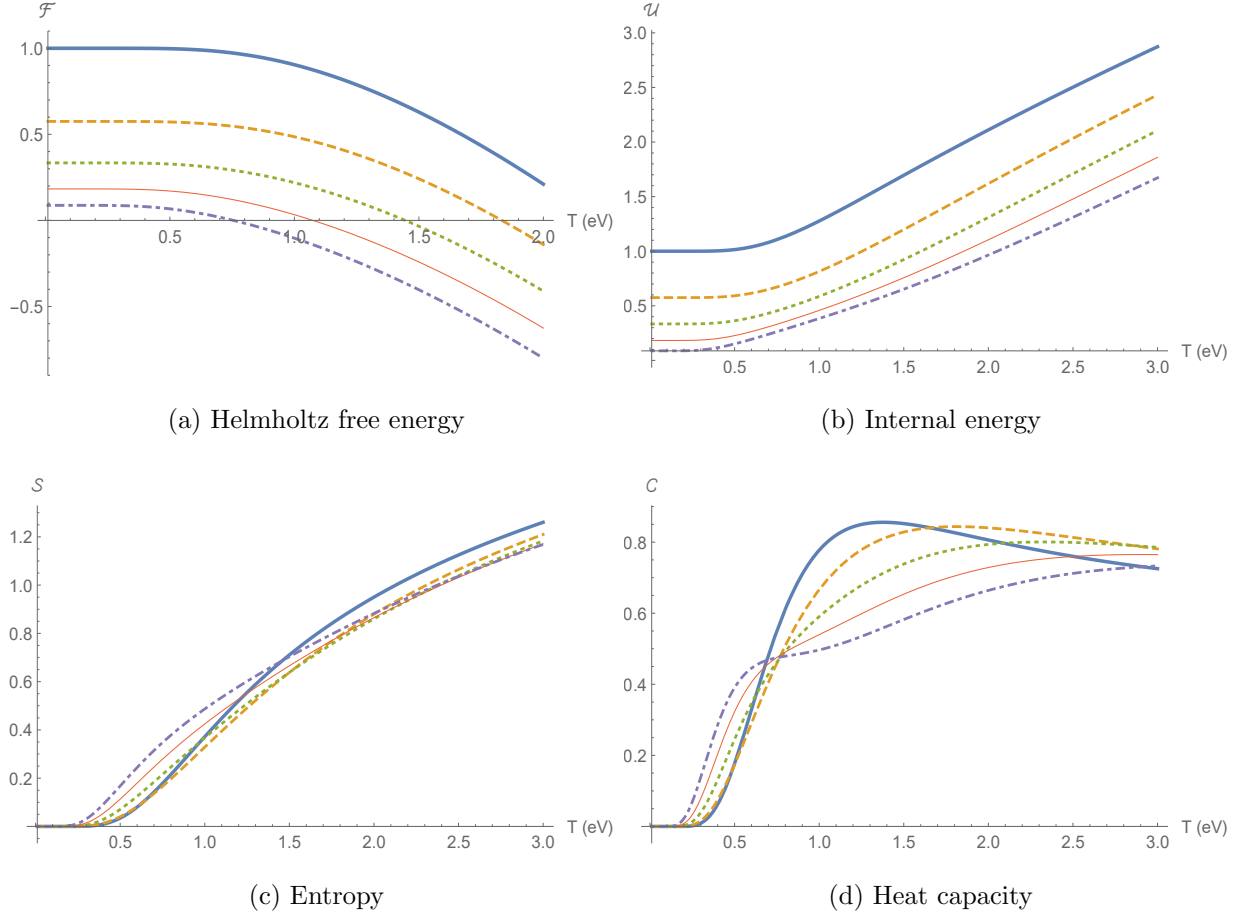


Figure 2: The thermodynamic behavior of Helmholtz free energy, internal energy, entropy and heat capacity, all modified by the isotropic parameter d_{00} , are presented. The plots can be identified using the labels as follows: (thick, blue, $\xi_{00} = 0.0$), (dashed, orange, $\xi_{00} = 0.3$), (dotted, green, $\xi_{00} = 0.6$), (thin, red, $\xi_{00} = 0.9$), (dotdashed, purple, $\xi_{00} = 1.2$).

Now, let us start with the Helmholtz free energy shown in Fig. 2a. The first feature is that the Helmholtz free energy decreases as parameter ξ_{00} increases. In this way, we conclude that the free energy is bounded from above for $\xi_{00} = 0$. We notice that as parameter ξ_{00} increases, the difference between energies, i.e., $\mathcal{F}(\xi_{00}) - \mathcal{F}(\xi_{00} + 0.3)$, decreases. We also see that the

influence of the parameter ξ_{00} persists for temperatures greater than those ones presented in Ref. 1a. Nevertheless, this influence vanishes whether we reach high temperatures. A similar behavior is verified for the internal energy, Fig. 2b. We detect that energy is a convex function of the temperature.

In particular, the behavior of entropy is exhibited in Fig. 2c. We note that such thermodynamic function is a concave function of temperature. Differently of what happened in the previous case, there is no value of parameter ξ_{00} that bounds the entropy either from above or below. The entropy tends to zero while the temperature goes to zero. For high temperature regime, the parameter ξ_{00} plays no role in such a case. In other words, the entropy assumes the same value no matter if ξ_{00} increases or decreases. We also observe that the entropy increases for $\xi_{00} > 0$.

Finally, we focus on the heat capacity encountered in Fig. 2d. For the high temperature regime, the heat capacity goes to 0.7, and, in the range $0 < T < 0.7$ eV, this thermodynamic function is a crescent function of the parameter ξ_{00} . However, this behavior changes if $T \approx 0.7$ eV. For $T > 0.7$ eV, the heat capacity is a decreasing function of ξ_{00} . It is important to notice that, at $\xi_{00} = 0$, the heat capacity has a maximum. We also see the convexity flattens as the parameter increases.

C. Spin currents

As we have already mentioned, we can also study the behavior of the spin current \mathcal{J}_φ^z as a function temperature. To do that, we need to consider the fluctuations of the canonical ensemble:

$$\begin{aligned}
\langle \mathcal{J}_\varphi^z \rangle &= \frac{1}{\mathcal{Z}_1} \sum_{n=0}^{\infty} \sum_{\{s,\lambda\}=\{\pm\}} \mathcal{J}_\varphi^z \exp(-\beta E_{n,s}^\lambda), \\
&= \frac{1}{\mathcal{Z}_1} \sum_{n=0}^{\infty} \sum_{\{s,\lambda\}=\{\pm\}} \frac{1}{4mr_0} (2n \cos \theta - 1) \exp(-\beta E_{n,s}^\lambda), \\
&= \frac{2 \cos \theta}{4mr_0} \frac{1}{\mathcal{Z}_1} \sum_{n=0}^{\infty} \sum_{\{s,\lambda\}=\{\pm\}} n \exp(-\beta E_{n,s}^\lambda) - \frac{1}{4mr_0}.
\end{aligned} \tag{29}$$

In Fig. 3, it is shown how z -component of spin currents behave for some values of temperature. Initially, let us analyze d_{ij} -case exhibited in Fig. 3a. Here, when $T > 0.2$ eV, the spin current is a decreasing function of ξ . Nevertheless, when $T < 0.2$ eV, something

unusual emerges.

On the other hand, for the range $0 < \xi < 0.6$, the spin current has its values diminished when parameter ξ increases. Nevertheless, when it overcomes $\xi = 0.6$, the behavior changes and \mathcal{J}_φ^z increases assuming a value greater than $\xi = 0.3$. Therefore, it recovers behavior of a decreasing function of ξ , with different range $0.7 < \xi < 1.2$ though.

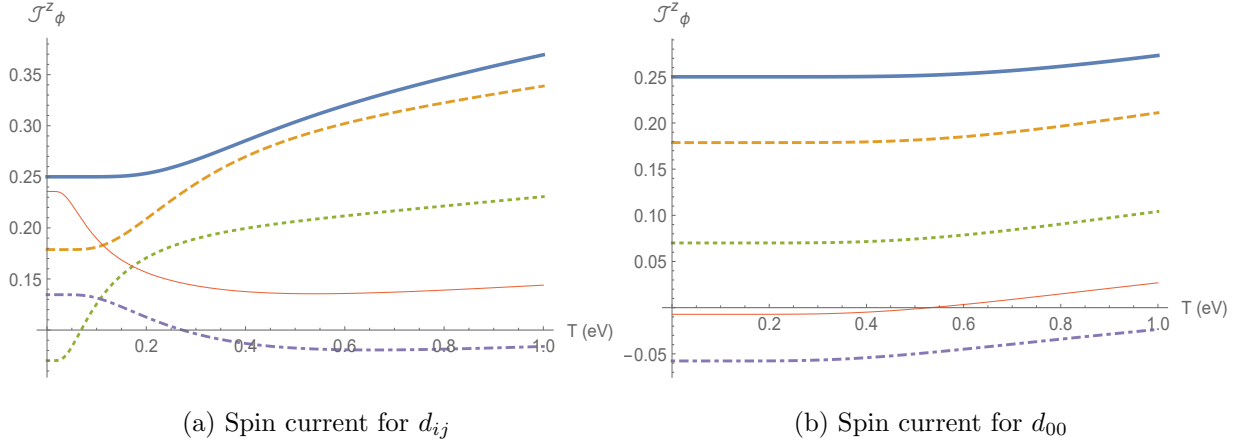


Figure 3: The spin currents results for the canonical approach are displayed above, where the labels (thick, blue, $\{\xi, \xi_{00}\} = 0.0$), (dashed, orange, $\{\xi, \xi_{00}\} = 0.3$), (dotted, green, $\{\xi, \xi_{00}\} = 0.6$), (thin, red, $\{\xi, \xi_{00}\} = 0.9$), (dotdashed, purple, $\{\xi, \xi_{00}\} = 1.2$) help us to identify the values choosed for the parameter ξ .

Now, let us study the implications of temperature and ξ at the current modified by d_{00} , see Fig. 3b. We observe at first that the current \mathcal{J}_φ^z is a function of temperature. We also realise the fact that the current is a decreasing function of ξ and the difference between two values of the current, that is $\mathcal{J}_\varphi^z(T, \xi_1) - \mathcal{J}_\varphi^z(T, \xi_2)$, is kept independent of the temperature. The difference in the behavior of the two cases displayed in Fig. 3 relies on the fact that the parameter d_{ij} induces an anisotropy in the space whereas the parameter d_{00} is isotropic.

IV. RESULTS FOR GRAND CANONICAL APPROACH

In this section, we present numerical analyses based on the grand canonical ensemble formalism. Particularly, we show the results for the particle number, internal energy, entropy and the heat capacity as a function of temperature and ξ . In what follows, the outcome results considering again d_{ij} and d_{00} are exhibited. Analogously to the previous section, we

finish our discussion, showing how z -component of the spin current interferes in our system as a function of the temperature.

A. Configuration d_{ij}

Let us start by looking, in Fig. 4a, how the particle number changes. We observe that $\mathcal{N}(T, \xi)$ is a convex function of temperature, i.e., it has a minimum. Another point is that the function $\mathcal{N}(T, \xi)$ turns out to have no dependence of ξ when high temperatures are taken into account. We also see that such thermal property is a decreasing function of ξ and the minimum is shifted to the left whether ξ increases. Notably, since particles are allowed to vary, we can use such a feat to control the number of electrons inside the ring.

Another important thermodynamic function is the internal energy, see Fig. 4b. We divide our analyses into two ranges, namely: $T \leq 0.4$ eV and $T > 0.4$ eV for a better comprehension. For the regime of temperature below $T = 0.4$ eV, we verify the following pattern: $\mathcal{U}(T, \xi = 0.6) < \mathcal{U}(T, \xi = 0.3) < \mathcal{U}(T, \xi = 0.9) < \mathcal{U}(T, \xi = 0) < \mathcal{U}(T, \xi = 1.2)$. On the other hand, for the range $T > 0.4$ eV, we realise that the internal energy is a increasing function of ξ .

The entropy is displayed in Fig. 4c. We see that entropy is a monotonic increasing function of the temperature. For $T = 0$, we observe that $\mathcal{S}(T = 0, \xi = 0) = 2$ and for $\mathcal{S}(T = 0, \xi \neq 0) = 0$. When we take into account the Lorentz violating parameter, the entropy has its value shifted to zero independent of ξ . We also conclude that $\mathcal{S}(T, \xi)$ tends to be parameter independent for high temperatures.

Finally, let us observe the heat capacity exhibited in Fig. 4d. We notice that a local maximum is formed when we regard the parameter ξ . We also observe that the heat capacity tends to 1.5 as temperature grows. The maximum value for the heat capacity is obtained for the configuration $\mathcal{C}(T = 0.4, \xi = 0.6)$.

B. Configuration d_{00}

Now, we intend to study the effects to the isotropic parameter d_{00} in the thermodynamic functions of the system. As we did before, we present the particle number in Fig. 5a. $\mathcal{N}(T, \xi)$ is a concave function of temperature and its local minimum is bounded from below

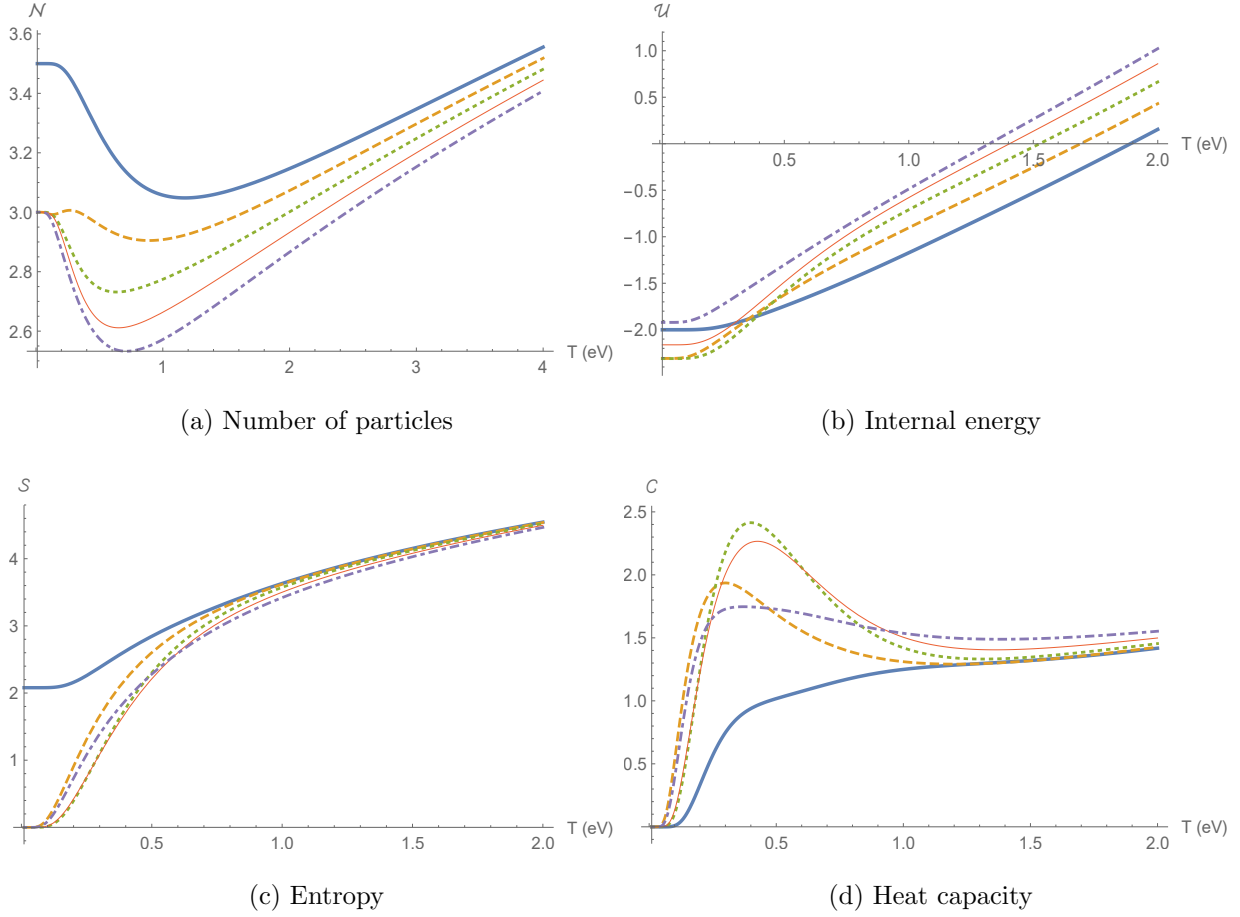


Figure 4: The main thermodynamic functions obtained by the grand canonical approach and modified by the anisotropic parameter d_{ij} are displayed above. The plots can be distinguished by the following labels: (thick, blue, $\xi = 0.0$), (dashed, orange, $\xi = 0.3$), (dotted, green, $\xi = 0.6$), (thin, red, $\xi = 0.9$), (dotdashed, purple, $\xi = 1.2$).

by the value $\xi = 0.9$. For high temperature regime, we observe the parameter ξ becoming negligible in the function $\mathcal{N}(T, \xi)$ when $T > 1.4$ eV. The minimum value is shifted to the left until it reaches $T \approx 0.63$ eV for $\xi = 0.9$. After this value, the minimum moves to the right again. We can use these information to control the number of particle inside the ring. Such a feature has many applications in nanotechnology [45–47].

To the internal energy, see Fig. 5b. We observe that, for high temperature regime, the parameter ξ become negligible and the function $\mathcal{U}(T, \xi)$ does not depend on ξ . For low temperature regime, mainly in the range $0 < T < 0.6$ eV, we observe an splitting in the energy. This means that the function $\mathcal{U}(T, \xi)$ is sensible to different values of ξ . Here,

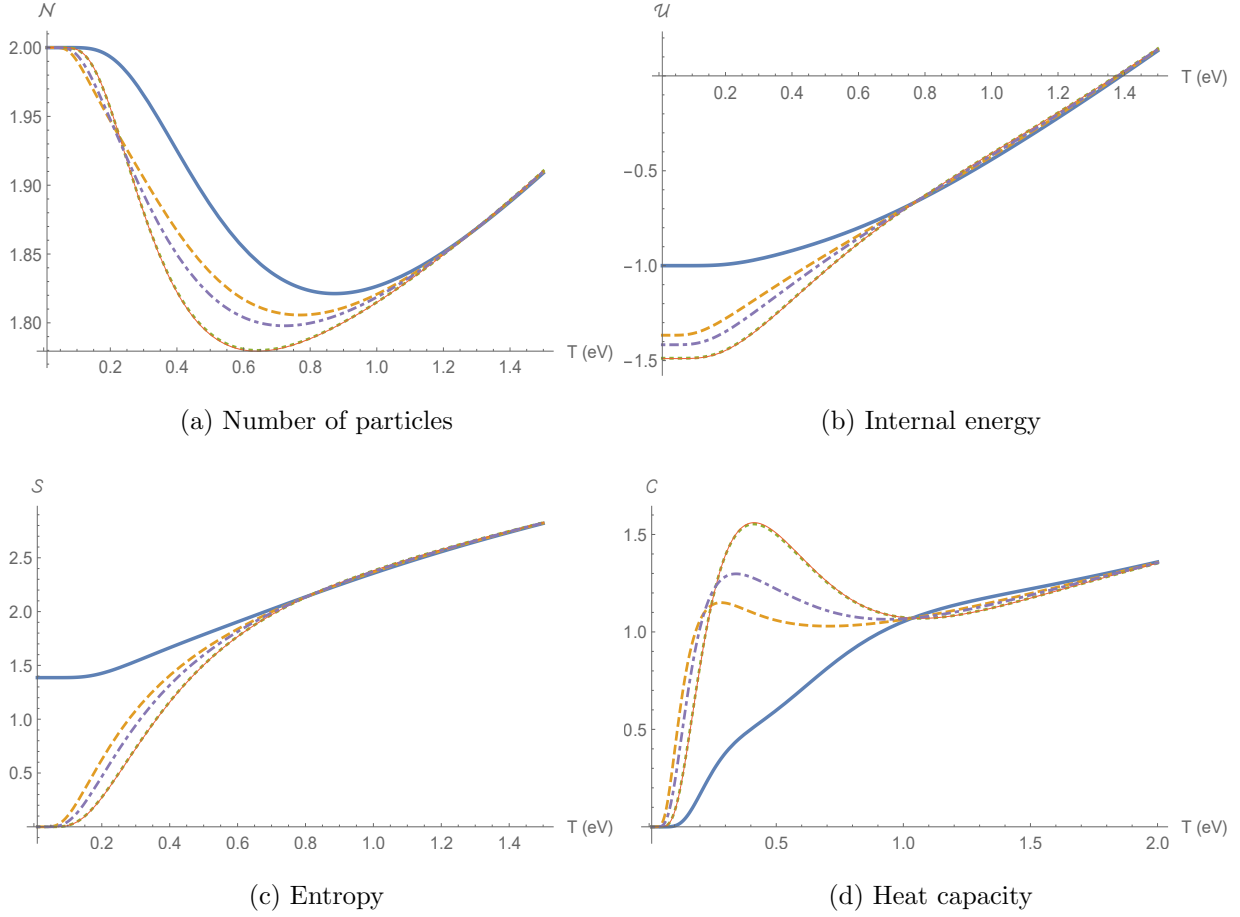


Figure 5: The thermodynamic behavior of Helmholtz free energy, internal energy, entropy and heat capacity, all modified by the isotropic parameter d_{00} , are showed above. The plots can be identified using the labels: (thick, blue, $\xi_{00} = 0.0$), (dashed, orange, $\xi_{00} = 0.3$), (dotted, green, $\xi_{00} = 0.6$), (thin, red, $\xi_{00} = 0.9$), (dotdashed, purple, $\xi_{00} = 1.2$).

the energy is bounded from below, and, for $\xi = 0.9$, and, for $\xi > 0.9$, the internal energy increases. For $T = 0$, we find that $-1.5 \text{ eV} < \mathcal{U}(T = 0, \xi) < -1.0 \text{ eV}$. The freedom in having to choose parameter ξ can also be of great importance in several applications, e.g., it controls the internal motions (kinetic energy) of electrons.

We finish this subsection by looking at the behavior of the heat capacity, which is shown in Fig. 5d. In agreement with what happens to the all thermodynamic functions studied in this manuscript, the heat capacity also becomes ξ independent if T reaches high values. There still exists a formation of a local maximum when we increase the values of ξ . More so, the maximum value reached by this local maximum is bounded from $\xi = 0.9$ and, for

$\xi > 0.9$. Remarkably, we can utilize conveniently ξ in order to maximize or even minimize the heat capacity of a quantum ring.

C. Spin currents

Here, we investigate the behavior of spin current when temperature is modified. To study it, we need to evaluate the mean value \mathcal{J}_φ^z with respect to the corresponding distribution of probability. In this sense, the average value of the spin current is given by

$$\langle \mathcal{J}_\varphi^z \rangle = \sum_{n=0}^{\infty} \sum_{\{s,\lambda\}=\{\pm\}} \frac{1}{4\pi r_0} \frac{(2n \cos \theta - 1)}{\exp [\beta (E_{n,s}^\lambda - \mu)] + 1}. \quad (30)$$

In order to analyze this expression numerically, we display the plots in Fig. 6 for both cases, namely, d_{ij} and d_{00} . $\mathcal{J}_\varphi^z(T, \xi)$ is a decreasing function of ξ up to $\xi = 0$ configuration. We also see that, for $\xi = 1.2$, electrons move in an opposite direction when compared to values in the range $0 \leq \xi \leq 0.6$. As mentioned in Ref. [59], the system can distinguish a clockwise and a counterclockwise moving current. We see that temperature has more influence under the counterclockwise motion for the anisotropic case. On the other hand, for the isotropic case, we observe that for $\xi = 1.2$ there is a turning point in the motion at $T = 0.15$ eV and electrons start moving clockwise.

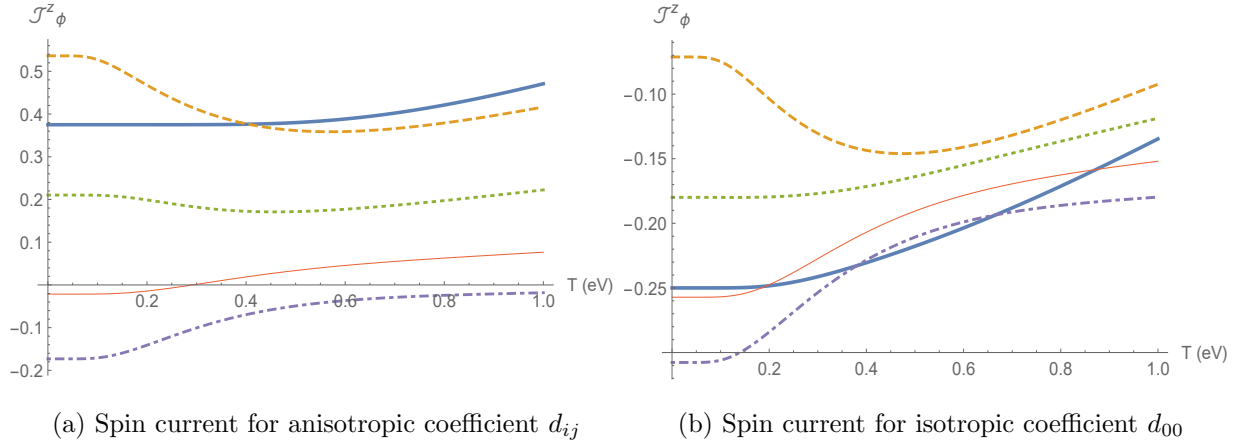


Figure 6: The spin currents results for the grand canonical approach are presented above, where the labels (thick, blue, $\{\xi, \xi_{00}\} = 0.0$), (dashed, orange, $\{\xi, \xi_{00}\} = 0.3$), (dotted, green, $\{\xi, \xi_{00}\} = 0.6$), (thin, red, $\{\xi, \xi_{00}\} = 0.9$), (dotdashed, purple, $\{\xi, \xi_{00}\} = 1.2$) identify the values of ξ .

Let us now examine how the internal energy, heat capacity, and spin currents change as the radius r_0 varies. In the upcoming plots, we compare two cases with a fixed temperature and different values for the Lorentz-violating coefficients. We begin by analyzing the internal energy, which is displayed in Fig. 7. It is interesting to note that in both cases, the internal energy reaches a local maximum before decreasing as the radius increases. Furthermore, for larger values of r_0 , the internal energy tends to stabilize and assume the same value. This is expected since the Lorentz violating coefficients become increasingly suppressed. Comparing the two cases, we see that the isotropic configuration produces a system with higher internal energy than the anisotropic one.

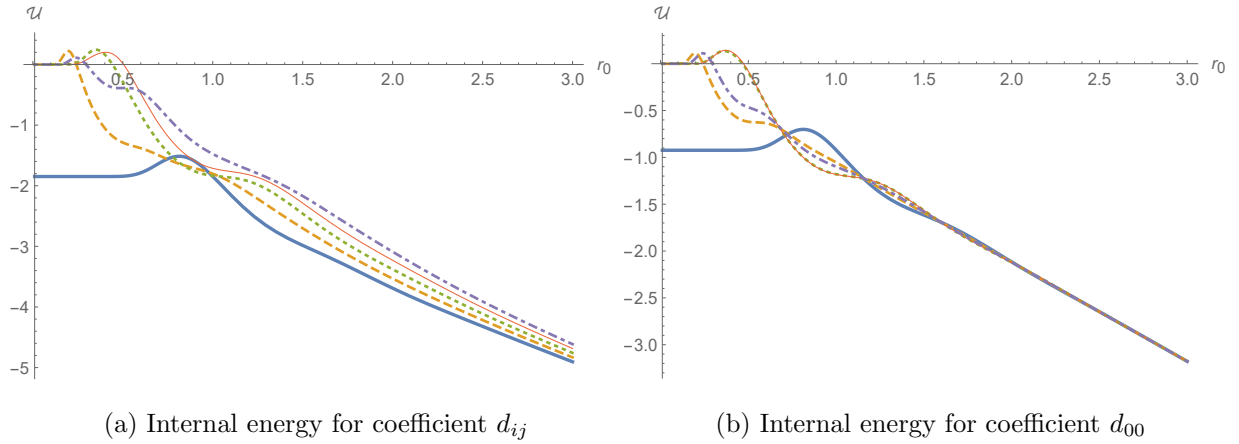


Figure 7: The internal energy for the grand canonical approach are presented above now as a function of r_0 , where the labels (thick, blue, $\{\xi, \xi_{00}\} = 0.0$), (dashed, orange, $\{\xi, \xi_{00}\} = 0.3$), (dotted, green, $\{\xi, \xi_{00}\} = 0.6$), (thin, red, $\{\xi, \xi_{00}\} = 0.9$), (dotdashed, purple, $\{\xi, \xi_{00}\} = 1.2$) identify the values of ξ for $T = 0.4$ eV.

In contrast to the internal energy, the heat capacity exhibits a periodic behavior as the radius increases, as shown in Fig. 8. For larger values of r_0 , the heat capacity tends to stabilize and assume the same value, which is expected due to the diminishing effects of Lorentz violation. Interestingly, the results for the anisotropic configuration produces a system with a larger heat capacity.

Finally, Fig. 9 illustrates the behavior of the spin current. It is evident that the magnitude of the spin current increases as the radius grows larger. Furthermore, a comparison of the two cases reveals that the anisotropic configuration produces a larger spin current.

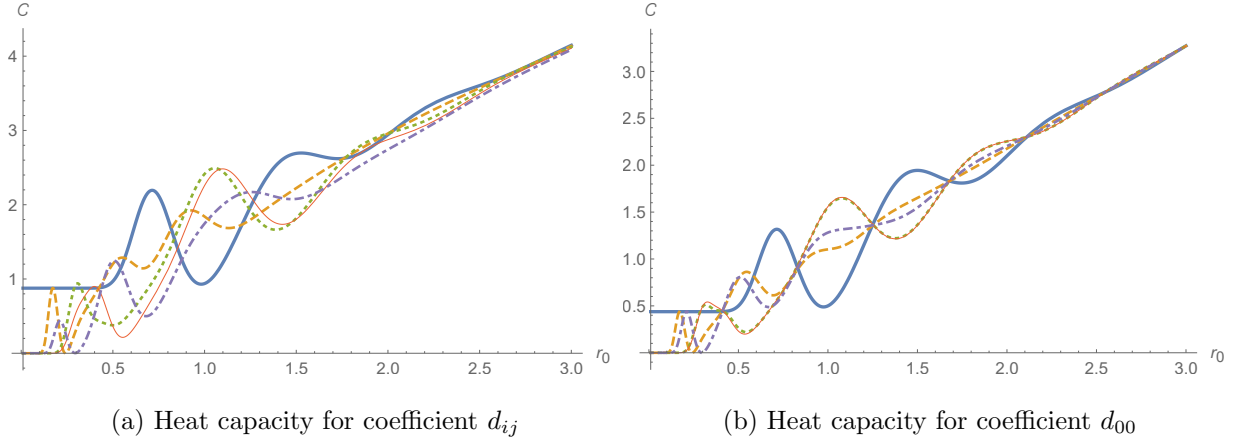


Figure 8: The Heat capacity for the grand canonical approach are presented above now as a function of r_0 , where the labels (thick, blue, $\{\xi, \xi_{00}\} = 0.0$), (dashed, orange, $\{\xi, \xi_{00}\} = 0.3$), (dotted, green, $\{\xi, \xi_{00}\} = 0.6$), (thin, red, $\{\xi, \xi_{00}\} = 0.9$), (dotdashed, purple, $\{\xi, \xi_{00}\} = 1.2$) identify the values of ξ for $T = 0.4$ eV.

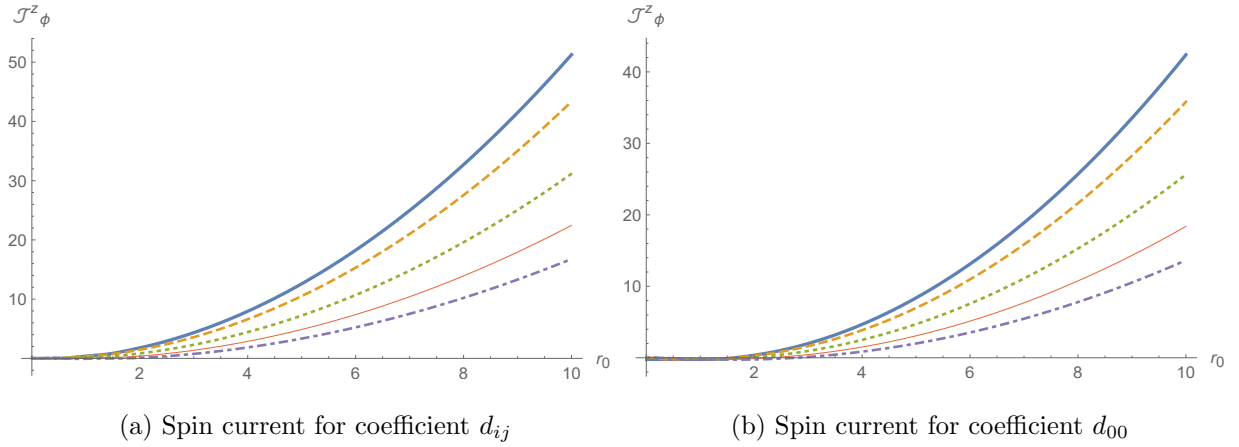


Figure 9: The spin current for the grand canonical approach are presented above now as a function of r_0 , where the labels (thick, blue, $\{\xi, \xi_{00}\} = 0.0$), (dashed, orange, $\{\xi, \xi_{00}\} = 0.3$), (dotted, green, $\{\xi, \xi_{00}\} = 0.6$), (thin, red, $\{\xi, \xi_{00}\} = 0.9$), (dotdashed, purple, $\{\xi, \xi_{00}\} = 1.2$) identify the values of ξ for $T = 0.4$ eV.

V. CONCLUSIONS

This manuscript had the purpose of calculating the thermodynamic properties of a quantum ring in the context of Lorentz violation. To do so, we fundamentally used the ensemble

approach.

Within the canonical ensemble, we calculated the partition functions for both operators d_{ij} and d_{00} . With these ones, we were able to calculate particle number, entropy, mean energy, heat capacity, and spin currents. In addition, we observed that parameter ξ played a major role at low temperature regime. In other words, the thermodynamic properties of a quantum ring turned out to be sensible to different values of ξ . Such a feature might probably be useful in the future nanotechnology in the case of the existence of Lorentz violation.

Another interesting property was related to the spin currents. In both scenarios, we saw that electrons could move clockwise or counterclockwise by choosing particular ranges of temperature and ξ . We noticed an inversion in their motion due to the change on Lorentz-violating parameters. When we compared the usual Rashba- and Dresselhauss-interactions, we realized that the controlling coefficients played the role of an external magnetic field.

As a future perspective, we could also examine the aforementioned properties, replacing electrons by other spin half particles or nanoparticles. These systems are now under consideration and they will appear in a forthcoming paper.

Acknowledgments

The authors also express their gratitude to FAPEMA, CNPq and CAPES (Brazilian research agencies) for invaluable financial support. In particular, J.A.A.S. Reis is supported by FAPEMA BPD-08734/22, L. Lisboa-Santos is supported by FAPEMA BPD-11962/22 and A. A. Araújo Filho is supported by Conselho Nacional de Desenvolvimento Científico e Tecnológico (CNPq) – 200486/2022-5. More so, the authors would like to thank the referees for their useful comments and suggestions given to us.

VI. DATA AVAILABILITY STATEMENT

Data Availability Statement: No Data associated in the manuscript

- [1] V. A. Kostelecký, R. Lehnert, and M. J. Perry, “Spacetime-varying couplings and lorentz violation,” *Physical Review D*, vol. 68, no. 12, p. 123511, 2003.
- [2] J. D. Tasson, “What do we know about lorentz invariance?,” *Reports on Progress in Physics*, vol. 77, no. 6, p. 062901, 2014.
- [3] D. Colladay and V. A. Kostelecký, “Lorentz-violating extension of the standard model,” *Physical Review D*, vol. 58, no. 11, p. 116002, 1998.
- [4] V. A. Kostelecký and M. Mewes, “Signals for lorentz violation in electrodynamics,” *Physical Review D*, vol. 66, no. 5, p. 056005, 2002.
- [5] V. A. Kostelecký, “Gravity, lorentz violation, and the standard model,” *Physical Review D*, vol. 69, no. 10, p. 105009, 2004.
- [6] V. A. Kostelecký and S. Samuel, “Spontaneous breaking of lorentz symmetry in string theory,” *Physical Review D*, vol. 39, no. 2, p. 683, 1989.
- [7] S. M. Carroll, G. B. Field, and R. Jackiw, “Limits on a lorentz-and parity-violating modification of electrodynamics,” *Physical Review D*, vol. 41, no. 4, p. 1231, 1990.
- [8] V. A. Kostelecký and M. Mewes, “Cosmological constraints on lorentz violation in electrodynamics,” *Physical Review Letters*, vol. 87, no. 25, p. 251304, 2001.
- [9] J. Alfaro, A. Andrianov, M. Cambiaso, P. Giacconi, and R. Soldati, “On the consistency of lorentz invariance violation in qed induced by fermions in constant axial-vector background,” *Physics Letters B*, vol. 639, no. 5, pp. 586–590, 2006.
- [10] C. Adam and F. R. Klinkhamer, “Causality and cpt violation from an abelian chern–simons-like term,” *Nuclear Physics B*, vol. 607, no. 1-2, pp. 247–267, 2001.
- [11] A. B. Scarpelli, H. Belich, J. Boldo, and J. Helayel-Neto, “Aspects of causality and unitarity and comments on vortexlike configurations in an abelian model with a lorentz-breaking term,” *Physical Review D*, vol. 67, no. 8, p. 085021, 2003.
- [12] R. Bluhm, V. A. Kostelecký, C. D. Lane, and N. Russell, “Clock-comparison tests of lorentz and cpt symmetry in space,” *Physical Review Letters*, vol. 88, no. 9, p. 090801, 2002.

- [13] J. Leite and T. Mariz, “Induced lorentz-violating terms at finite temperature,” *Europhysics Letters*, vol. 99, no. 2, p. 21003, 2012.
- [14] J. Leite, T. Mariz, and W. Serafim, “The induced higher derivative lorentz-violating chern–simons term at finite temperature,” *Journal of Physics G: Nuclear and Particle Physics*, vol. 40, no. 7, p. 075003, 2013.
- [15] J. Furtado and T. Mariz, “Lorentz-violating euler-heisenberg effective action,” *Physical Review D*, vol. 89, no. 2, p. 025021, 2014.
- [16] J. Assunção and T. Mariz, “Radiatively induced cpt-odd chern-simons term in massless qed,” *Europhysics Letters*, vol. 110, no. 4, p. 41002, 2015.
- [17] A. Ferrari, J. Furtado, J. Assunção, T. Mariz, and A. Y. Petrov, “One-loop calculations in lorentz-breaking theories and proper-time method,” *Europhysics Letters*, vol. 136, no. 2, p. 21002, 2022.
- [18] M. Schreck, “Analysis of the consistency of parity-odd nonbirefringent modified maxwell theory,” *Physical Review D*, vol. 86, no. 6, p. 065038, 2012.
- [19] V. A. Kostelecký and M. Mewes, “Electrodynamics with lorentz-violating operators of arbitrary dimension,” *Physical Review D*, vol. 80, no. 1, p. 015020, 2009.
- [20] C. Reyes, L. Urrutia, and J. Vergara, “Quantization of the myers-pospelov model: The photon sector interacting with standard fermions as a perturbation of qed,” *Physical Review D*, vol. 78, no. 12, p. 125011, 2008.
- [21] R. Bluhm, V. A. Kostelecký, and C. D. Lane, “Cpt and lorentz tests with muons,” *Physical Review Letters*, vol. 84, no. 6, p. 1098, 2000.
- [22] V. A. Kostelecký, R. Lehnert, and M. J. Perry, “Spacetime-varying couplings and lorentz violation,” *Physical Review D*, vol. 68, no. 12, p. 123511, 2003.
- [23] S. Kruglov, “Modified dirac equation with lorentz invariance violation and its solutions for particles in an external magnetic field,” *Physics Letters B*, vol. 718, no. 1, pp. 228–231, 2012.
- [24] R. Lehnert, “Threshold analyses and lorentz violation,” *Physical Review D*, vol. 68, no. 8, p. 085003, 2003.
- [25] B. Goncalves, Y. N. Obukhov, and I. L. Shapiro, “Exact foldy-wouthuysen transformation for a dirac spinor in torsion and other c p t and lorentz violating backgrounds,” *Physical Review D*, vol. 80, no. 12, p. 125034, 2009.
- [26] V. A. Kostelecký and M. Mewes, “Fermions with lorentz-violating operators of arbitrary di-

- mension,” *Physical Review D*, vol. 88, no. 9, p. 096006, 2013.
- [27] J. Reis *et al.*, “Thermal aspects of interacting quantum gases in lorentz-violating scenarios,” *The European Physical Journal Plus*, vol. 136, no. 3, pp. 1–30, 2021.
 - [28] R. Winkler, *Spin-orbit coupling effects in two-dimensional electron and hole systems*, vol. 191. Springer, 2003.
 - [29] K. Y. Bliokh, F. J. Rodríguez-Fortuño, F. Nori, and A. V. Zayats, “Spin–orbit interactions of light,” *Nature Photonics*, vol. 9, no. 12, pp. 796–808, 2015.
 - [30] V. A. Kostelecký and N. Russell, “Data tables for lorentz and c p t violation,” *Reviews of Modern Physics*, vol. 83, no. 1, p. 11, 2011.
 - [31] D. Colladay and P. McDonald, “Statistical mechanics and lorentz violation,” *Physical Review D*, vol. 70, no. 12, p. 125007, 2004.
 - [32] A. A. Araújo Filho and R. V. Maluf, “Thermodynamic properties in higher-derivative electrodynamics,” *Brazilian Journal of Physics*, vol. 51, no. 3, pp. 820–830, 2021.
 - [33] M. Anacleto, F. Brito, E. Maciel, A. Mohammadi, E. Passos, W. Santos, and J. Santos, “Lorentz-violating dimension-five operator contribution to the black body radiation,” *Physics Letters B*, vol. 785, pp. 191–196, 2018.
 - [34] R. C. Myers and M. Pospelov, “Ultraviolet modifications of dispersion relations in effective field theory,” *Physical Review Letters*, vol. 90, no. 21, p. 211601, 2003.
 - [35] T. Mariz, J. Nascimento, and A. Y. Petrov, “Perturbative generation of the higher-derivative lorentz-breaking terms,” *Physical Review D*, vol. 85, no. 12, p. 125003, 2012.
 - [36] A. A. Araújo Filho, “Lorentz-violating scenarios in a thermal reservoir,” *The European Physical Journal Plus*, vol. 136(4), 417 (2021).
 - [37] R. Casana, M. M. Ferreira Jr, and J. S. Rodrigues, “Lorentz-violating contributions of the carroll-field-jackiw model to the cmb anisotropy,” *Physical Review D*, vol. 78, no. 12, p. 125013, 2008.
 - [38] R. Casana, M. M. Ferreira Jr, J. S. Rodrigues, and M. R. Silva, “Finite temperature behavior of the c p t-even and parity-even electrodynamics of the standard model extension,” *Physical Review D*, vol. 80, no. 8, p. 085026, 2009.
 - [39] A. A. Araújo Filho and A. Y. Petrov, “Higher-derivative lorentz-breaking dispersion relations: a thermal description,” *The European Physical Journal C*, vol. 81(9), 843 (2021).
 - [40] A. A. Araújo Filho, “Thermodynamics of massless particles in curved spacetime,” *arXiv*

preprint *arXiv:2201.00066*, 2021.

- [41] A. A. Araújo Filho and A. Y. Petrov, “Bouncing universe in a heat bath,” *International Journal of Modern Physics A*, vol. 36, p. 2150242, 2021.
- [42] A. A. Araújo Filho, “Particles in loop quantum gravity formalism: a thermodynamical description,” *Annalen der Physik*, p. 2200383, 2022.
- [43] R. Khordad and H. R. Sedehi, “Thermodynamic properties of a double ring-shaped quantum dot at low and high temperatures,” *Journal of Low Temperature Physics*, vol. 190, no. 3, pp. 200–212, 2018.
- [44] R. R. Oliveira, A. A. Araújo Filho, F. C. Lima, R. V. Maluf, and C. A. Almeida, “Thermodynamic properties of an aharonov-bohm quantum ring,” *The European Physical Journal Plus*, vol. 134, no. 10, p. 495, 2019.
- [45] T. Chakraborty and P. Pietiläinen, “Electron-electron interaction and the persistent current in a quantum ring,” *Physical Review B*, vol. 50, no. 12, p. 8460, 1994.
- [46] R. J. Warburton, C. Schäfflein, D. Haft, F. Bickel, A. Lorke, K. Karrai, J. M. Garcia, W. Schoenfeld, and P. M. Petroff, “Optical emission from a charge-tunable quantum ring,” *Nature*, vol. 405, no. 6789, pp. 926–929, 2000.
- [47] A. Fuhrer, S. Lüscher, T. Ihn, T. Heinzel, K. Ensslin, W. Wegscheider, and M. Bichler, “Energy spectra of quantum rings,” *Nature*, vol. 413, no. 6858, pp. 822–825, 2001.
- [48] K. Bakke and H. Belich, “On the lorentz symmetry breaking effects on a dirac neutral particle inside a two-dimensional quantum ring,” *The European Physical Journal Plus*, vol. 129, 147 (2014).
- [49] K. Bakke and H. Belich, “On the influence of a rashba-type coupling induced by lorentz-violating effects on a landau system for a neutral particle,” *Annals of Physics*, vol. 354, pp. 1–9, 2015.
- [50] R. Casana, M. Ferreira Jr, V. Mouchrek-Santos, and E. O. Silva, “Generation of geometrical phases and persistent spin currents in 1-dimensional rings by lorentz-violating terms,” *Physics Letters B*, vol. 746, pp. 171–177, 2015.
- [51] V. A. Kostelecký and R. Lehnert, “Stability, causality, and lorentz and cpt violation,” *Physical Review D*, vol. 63, no. 6, p. 065008, 2001.
- [52] A. A. Araújo Filho, J. Reis, and S. Ghosh, “Fermions on a torus knot,” *The European Physical Journal Plus*, vol. 137(5), 614 (2022).

- [53] R. Oliveira, A. A. Araújo Filho, R. Maluf, and C. Almeida, “The relativistic aharonov–bohm–coulomb system with position-dependent mass,” *Journal of Physics A: Mathematical and Theoretical*, vol. 53, no. 4, p. 045304, 2020.
- [54] R. Oliveira, A. A. Araújo Filho, R. Maluf, and C. Almeida, “Reply to comment on ‘the relativistic aharonov–bohm–coulomb system with position-dependent mass’,” *Journal of Physics A: Mathematical and Theoretical*, vol. 54, no. 2, p. 028002, 2020.
- [55] R. Oliveira *et al.*, “Thermodynamic properties of neutral dirac particles in the presence of an electromagnetic field,” *The European Physical Journal Plus*, vol. 135(1), 99 (2020).
- [56] V. Kac and P. Cheung, “Euler-maclaurin formula,” in *Quantum Calculus*, pp. 92–98, Springer, 2002.
- [57] Z. M. C. Z. Y. Y. J. C. Y. Wang, Jianli; Wu, “Effect of electrical contact resistance on measurement of thermal conductivity and wiedemann-franz law for individual metallic nanowires,” *Scientific Reports*, vol. 8, p. 4862, Mar 2018.
- [58] D. Kojda, R. Mitdank, M. Handweg, A. Mogilatenko, M. Albrecht, Z. Wang, J. Ruhhammer, M. Kroener, P. Woias, and S. F. Fischer, “Temperature-dependent thermoelectric properties of individual silver nanowires,” *Phys. Rev. B*, vol. 91, p. 024302, Jan 2015.
- [59] B. Berche, C. Chatelain, and E. Medina, “Mesoscopic rings with spin-orbit interactions,” *European journal of physics*, vol. 31, no. 5, p. 1267, 2010.